Physics

Electricity & Magnetism fields

Okayama University *Year* 1998

Effect of minor loop on magnetic characteristics of permanent magnet type of MRI

Norio Takahashi* Takeshi Kayano†

Koji Miyata‡ Ken Ohashi**

*Okayama University

†Okayama University

‡Shin-Etsu Chemical Corporation Limited

**Shin-Etsu Chemical Coporation Limited

This paper is posted at eScholarship@OUDIR : Okayama University Digital Information Repository.

http://escholarship.lib.okayama-u.ac.jp/electricity_and_magnetism/19

Effect of Minor Loop on Magnetic Characteristics of Permanent Magnet Type of MRI

Norio Takahashi and Takeshi Kayano
Department of Electrical and Electronic Engineering
Okayama University, Okayama 700-8530, Japan

Koji Miyata and Ken Ohashi
Magnetic Materials R&D Center
Shin-Etsu Chemical Co. Ltd., Takefu 915-0802, Japan

Abstract **- A modeling technique of minor loop using typical hysteresis loops is shown. The effect of minor loop and eddy current in pole piece of a permanent magnet type of MRI on the residual flux density of probe coil is examined. It is illustrated that the change ΔB of residual flux density occurs due to the minor loop of pole piece. It is also pointed out that the choice of time interval Δt is important in the nonlinear analysis considering minor loop.**

Index terms **- Hysteresis, minor loop, MRI, finite element method**

I. Introduction

The permanent magnet type of MRI [1] for whole body provides a viable alternative to resistive and superconducting MRI [2]. As the permanent magnet assembly contains pole pieces and yokes which are made of steel, the minor loop of B and H of steel due to the pulse excitation and the eddy current induced in the steel affect the magnetic characteristics of permanent magnet assembly [3].

In this paper, the nonlinear iteration method for the analysis considering minor loop is discussed, and also the modeling technique of minor loop using typical major hysteresis loops is shown. The behavior of magnetic characteristics of permanent magnet assembly is examined considering hysteresis and eddy current.

II. Analyzed Model

Fig. 1 shows the cross-section of a permanent magnet assembly for MRI device. The yoke is composed of two steel plates (530mm), other two steel plates (ϕ330mm) with a hole (ϕ60mm) and four columns. The permanent magnet has a hole (ϕ60mm). Although the actual assembly is three-dimensional having four columns, it is simplified to a two-dimensional one to reduce the CPU time and memory requirements. The yoke and pole piece are made of steel (SS400), and its conductivity is 7.51×10^6S/m. The magnetization of Nd-Fe-B magnet is 1.21 T. The gradient coil having 15 turns is located on the surface of the pole piece.

Fig. 2 shows the current of the gradient coil. The flux density B in this model is produced by the permanent magnet and the gradient coil. Therefore, B and H are located on the initial magnetization curve and on the minor loop.

Manuscript received June 3, 1998
N. Takahashi, tel: +81-86-251-8115, fax: +81-86-251-8258
e-mail: norio@eplab.elec.okayama-u.ac.jp

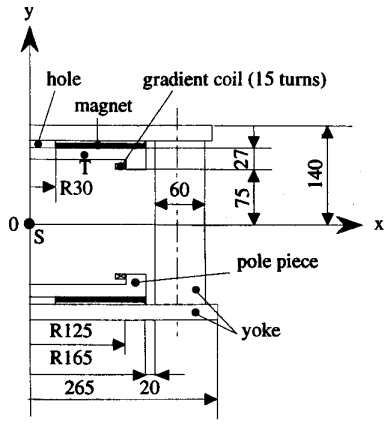

Fig. 1. Model of permanent magnet assembly for MRI device.

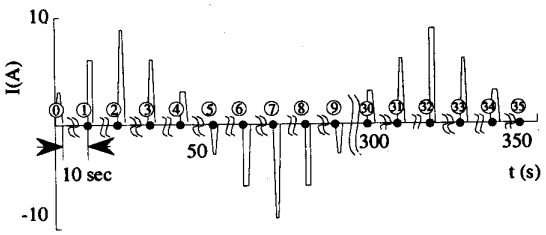

(a) pulse series

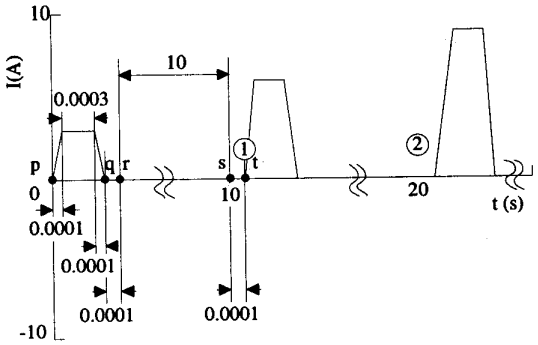

(b) enlarged pulse series

Fig. 2. Current of gradient coil.

0018-9464/99$10.00 © 1999 IEEE

III. Method Of Analysis

A. Choice of B-H curve in Newton-Raphson Iteration

The choice of minor loop in the Newton-Raphson nonlinear iteration (NR method) is carried out as follows:

(a) Let us assume that B and H at a step is located at the point a on the initial magnetization curve ① shown in Fig. 3. If the obtained flux density $B_1^{t(k)}$ of the k-th iteration at the instant t is larger than $B_1^{(t-\Delta t)(k)}$ at the instant t-Δt, the operating point of B and H exists on the initial magnetization curve ①.

(b) If the flux density $B_1^{t(k)}$ is reduced ($B_1^{t(k)}<B_1^{(t-\Delta t)(k)}$), the operating point of B and H moves on the upper minor loop ② as shown in Fig. 3. In Fig. 3, the case when the operating point is reached to the point b($B_1^{t(3)}$) after three NR iterations ($B_1^{t(1)}>B_1^{t(2)}>B_1^{t(3)}$) is shown.

(c) When the flux density $B_1^{t(k)}$ at the k-th step (k>3) of NR method is larger than B_1^{t}, $B_1^{t(k)}$ moves on the lower minor loop ③ shown in Fig. 3. In the NR iteration, the operating point moves on loop ⑤ when B is reduced, the operating point moves on loop ③ when B is increased.

(d) If the operating point is located at the point h on the lower loop in Fig. 3, the operating point moves on small upper minor loop ④ and upper hysteresis loop ⑤ when B is reduced, and the operating point moves on loop ③ when B is increased.

B. Modeling of Minor Loop

The upper and lower minor loops can be determined as follows:

1) Upper minor loop: The upper minor loop ② is represented by the upper hysteresis loop shown in Fig. 4, which is approximated by a cubic spline function. Typical hysteresis loops are measured using a permeameter [4]. The specimen is steel 'SS400' and the dimension is 10×50×300mm. The upper hysteresis loop used is interpolated by the measured loops which are stored as follows:

(a) The upper loop "2" having the maximum flux density B_{m2} shown in Fig. 5 is interpolated from two nearest typical loops "1" and "3" satisfying the following relationship:

$$\frac{\overline{P'P}}{\overline{PP''}} = \frac{\overline{P_1P_2}}{\overline{P_2P_3}} \tag{1}$$

(b) If the required loop is smaller than the smallest loop which is stored, the required loop is obtained by scaling down the smallest one similarly.

(c) If the required flux density is larger than that of the largest loop, the initial curve is used.

The small upper minor loop ④ which was denoted in Section III.A.(d) can be obtained from the lower minor loop b-h in the same way that the lower minor loop ③ is obtained from the upper minor loop ② as shown in the following Section III.*B.2)*.

2) Lower minor loop: The lower minor loop ③ is obtained from the upper minor loop ②, assuming that the lower loop is symmetric with the upper one with respect to the middle point of the line a-b.

Fig.6 shows the comparison of simulated minor loop and measured minor loop. The minor loop of steel is measured using a permeameter. The calculated minor loop is obtained using the curves in Fig. 4. Fig. 6 suggests the validity of the modeling method of minor loop.

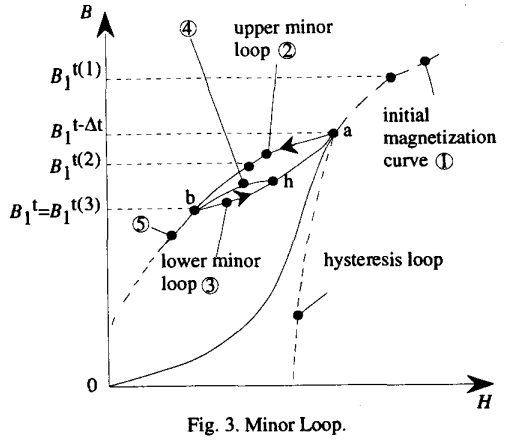

Fig. 3. Minor Loop.

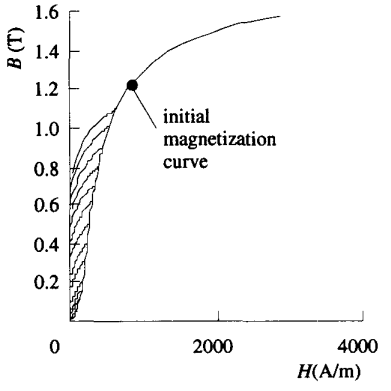

Fig. 4. Measured upper hysteresis loops (steel).

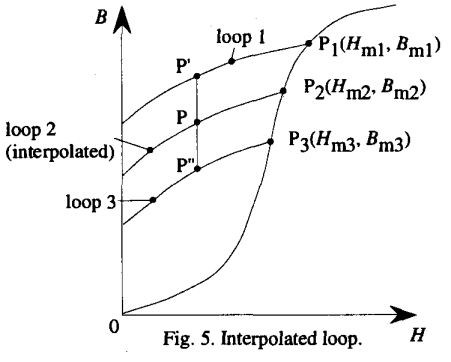

Fig. 5. Interpolated loop.

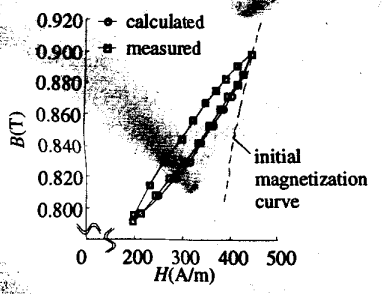

Fig. 6. Simulated and measured minor loops.

IV. Results And Discussion

A. Flux Density

Fig.7 shows the operating points of $|B|$ and $|H|$ on the initial magnetization curve and minor loops at the point T (70,88) in the pole piece shown in Fig. 1. The range of minor loop is changed due to eddy current.

Fig. 8 shows the time variation of the z-component B_z of flux density at the point S(0,0) in the gap. The abscissa denotes the time step. The selection of time interval Δt is important in the nonlinear analysis taking account of minor loop. When Δt is chosen as 2 sec during all period of q-t in Fig. 2, the NR iteration was not converged. Therefore, the time increment Δt is chosen as 10^{-5} sec during the period of p-q-r, 2 sec during r-s and 10^{-5} sec during s-t. This may because the change of flux density becomes to large when large Δt is chosen. The difference between the ordinary nonlinear analysis without minor loop and the present analysis with minor loop is that the operating point of B and H moves on the loops having large different slopes, for example, between the upper minor loop ② and the lower minor loop ③. The introduction of the relaxation factor α [5] as shown in the following equation is necessary in the nonlinear analysis taking account of minor loop:

$$A^{k+1} = A^k + \alpha \delta A^k \qquad (2)$$

where A^k is the vector potential at the k-th iteration. δA^k is the increment of A. In this case, α is chosen as 0.5. Table I shows the discretization data and CPU time.

Fig. 9 shows the change of flux density B_z with time at the point S(0,0). The flux densities at the instants ①, ②,•••, when the current becomes equal to zero and the transient phenomenon of current is finished, are plotted. The flux density with eddy current is smaller than that without eddy current due to the opposing magnetic field produced by the eddy current.

Table I Discretization data and CPU time

	without eddy current	with eddy current
number of elements	4409	
number of nodes	2246	
number of NR interations (at step 1)	7	6
number of time steps	2625	
CPU time (h)	1.3	2.1

Computer used : IBM3AT(49.7 MFLOPS)
Convergence criterion for NR iteration : $\Delta B = 1 \times 10^{-7}$ (T)

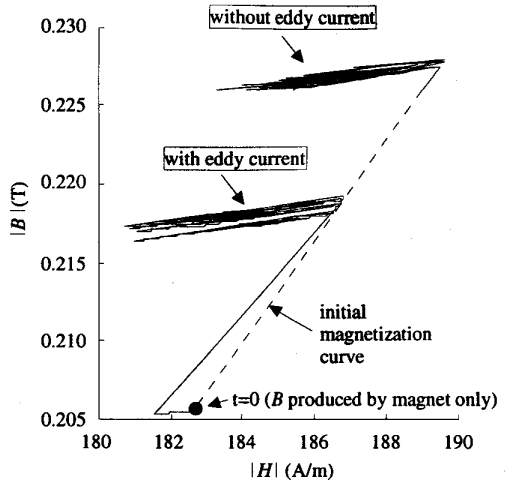

Fig. 7. B and H on minor loop (point T in pole piece).

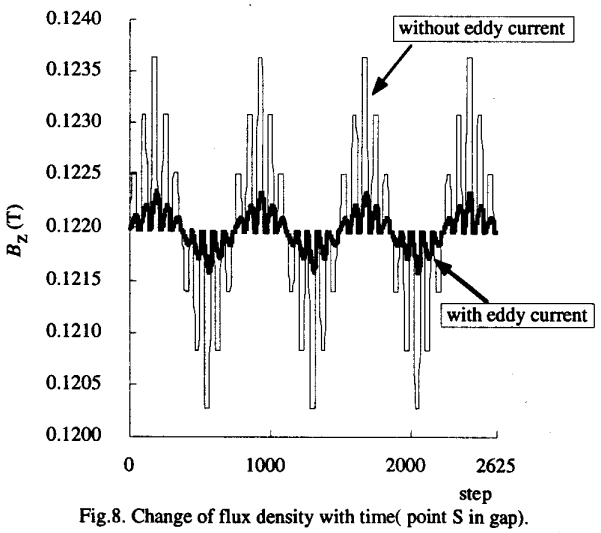

Fig.8. Change of flux density with time(point S in gap).

B. Change of Residual Flux Density

The change ΔB_z of residual flux density at the point S(0,0) in the gap is examined. ΔB_z corresponds to the output of the probe coil of MRI. ΔB_z is given by

$$\Delta B_z = B_{zi} - B_{z0} \qquad (3)$$

where B_{z0} is the flux density at the instant t=0 (I=0A). B_{zi} is the flux density at the instant t=i (I=0A) shown in Fig. 2. If there is no eddy current and no minor loop in the pole piece,

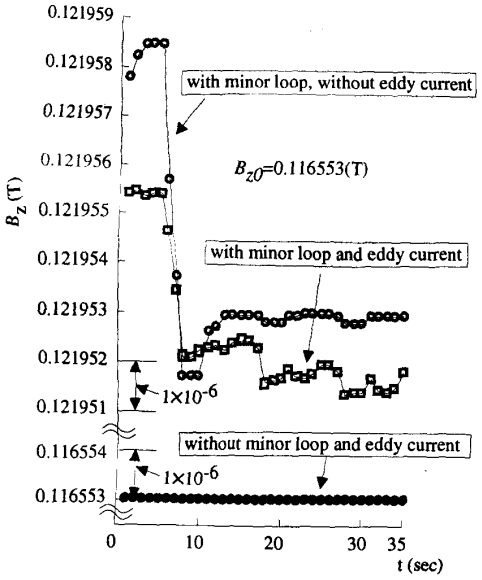

Fig. 9. Flux densities at instants ①, ② etc (point S in gap).

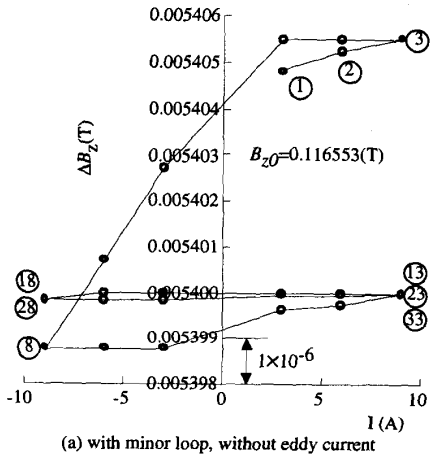

(a) with minor loop, without eddy current

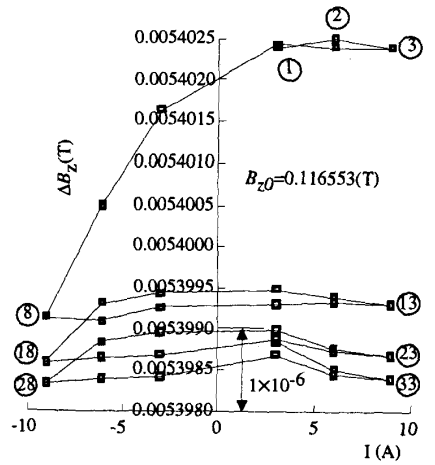

(a) with minor loop and eddy current

Fig. 10. Change of residual flux density.

ΔB_z is always equal to zero, because B_z does not change with time.

Fig. 10 shows the change ΔB_z of residual flux density with time. The tendency of the shape of locus of ΔB_z is not so much different from the measured one. Figs. 9 and 10 suggest that the major cause for the residual flux density is the minor loop, and the shape of locus of ΔB_z is affected by the eddy current.

CONCLUSIONS

The obtained results can be summarized as follows:

(1) The minor loop can be represented using upper hysteresis loop, and the validity of the modeling of minor loop is shown by comparing with measurement.

(2) The selection of time interval Δt is important in the nonlinear analysis taking account of minor loop.

(3) The change ΔB_z of residual flux density is produced due to the minor loop of pole piece.

Although the tendency of the shape of locus of ΔB_z is not so much different from the measured one, a more precise analysis taking account of multi-minor loops, namely many minor loops occur in a minor loop, should be carried out.

REFERENCES

[1] T.Miyamoto, H.Sakurai, H.Takabayashi and M.Aoki, "A development of a permanent magnet assembly for MRI devices using Nd-Fe-B material", *IEEE Trans. Magn.*, vol.25, no.5, pp.3907-3909, Sept. 1989.

[2] P.R.Locher, "Proton NMR tomography", *Philips Technical Review*, vol.41, no.3, pp.73-88, 1983/84.

[3] K.Miyata, K.Ohashi, N.Takahashi and H.Ukita, "Analysis of magnetic characteristics of permanent magnet assembly for MRI devices taking account of hysteresis and eddy current", *IEEE Trans. Magn.*, vol.34, no.5, 1998.

[4] IEC, "Method of measurement of the d.c. magnetic properties of solid steels in a closed magnetic circuit", 404-4 TC68 WG2 N63, Sept., 1991.

[5] K.Fujiwara, T.Nakata and N.Okamoto, "Method for determining relaxation factor for modified Newton-Raphson method", *IEEE Trans. Magn.*, vol.29, no.2, pp.1962-1965, March 1993.